JOURNAL OF CATALYSIS 21, 130–138 (1971)

Sulfiding of Nickel Catalyst Beds

JAMES T. RICHARDSON*

Synthetic Fuels Research Laboratory, Esso Research and Engineering, Baytown, Texas 77520

Received July 10, 1970

A moving coil permeameter has been used to confirm that sulfided nickel catalyst beds obey the Bohart–Adams poisoning wave equation. Poisoning by H_2S at low velocities (<20 cm/sec) is reaction limited at low temperatures (<150°C), mass transfer limited at intermediate temperatures (150–300°C) and controlled by solid phase diffusion at higher temperatures (>300°C); CS_2 and $(C_2H_5)_2S$ are mass transfer controlled up to 300°C. Thiophene is adsorption limited.

Sulfided catalysts are regenerable for guard chamber performance (except in the case of thiophene) but retain a layer of surface sulfide which effectively poisons catalytic activity. Regeneration above 600°C deactivates the catalyst for sulfur removal as well as hydrogenation.

Introduction

Process streams for hydrogenation reactions over nickel catalysts often contain traces of sulfur compounds which poison the catalyst. The nickel at the front of the bed is sulfided in a mass transfer zone which moves down the reactor with increasing process time. Process designers sometimes take advantage of this zone sulfiding by incorporating nickel guard chambers ahead of the main reactor.

Both the prediction of reactor performance and the design of guard chambers is greatly facilitated if the mechanism and kinetics for sulfur removal are known and may be extrapolated to process conditions. Several authors have reviewed the theories of adsorption and ion-exchange columns (*1–3*). The usual practice is to substantiate the theories and characterize the parameters through examination of the breakthrough curves. Determinations of concentration profiles in the bed itself have not been reported with sufficient accuracy to yield meaningful information.

This paper describes a moving coil permeameter designed to measure nickel concentration profiles in catalyst beds. The application of this technique to mechanistic and kinetic measurements in adsorption beds is also demonstrated.

* Present address: Department of Chemical Engineering, University of Houston, Houston, Texas 77004.

Experimental Methods

1. Moving Coil Permeameter

The principle of the permeameter is identical to that described by Selwood (*4*) except that high temperature measurements are possible and the secondary coil is movable over the catalyst bed. Figure 1 shows the essential features of the design.

The primary coil is made from 10,000 turns of Alfa No. HF24 magnet wire, wound in 14 layers on a brass form 12 in. long. Copper cooling coils allow sufficient cooling when the primary voltage is 120 volts ac. The working area is a 2-in. diameter tube 12 in. in length. The glass heating unit fits into this volume. The inner tube of this unit is made from a section of 19-mm o.d. Pyrex E-C coated conducting-tubing. This tubing is connected to a variable ac voltage through a Variac and is the heating element for the unit. The outer 5-cm o.d. tube provides either an evacuated insulating space to protect the primary

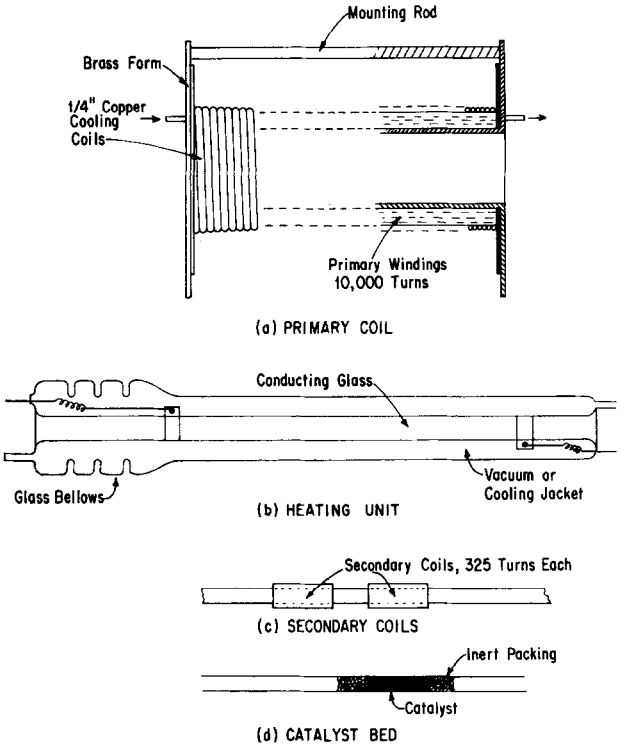

FIG. 1. Details of the moving coil permeameter for measuring nickel concentration profiles.

coil or a cooling channel to remove heat of reaction during room temperature exothermic reactions. The glass bellows allow for thermal expansion due to temperature differences between the inner and outer tubes. This device is operable up to 400°C.

The secondary unit has two coils connected in a differential mode, i.e., the net secondary output depends only on the difference in permeability between the materials surrounded by the coils. Each coil is 5 cm in length and is made from 0.01 in. oxygen-free silver wire with Type "D" MgO insulation. This wire is manufactured by the Secon Metals Corporation and tolerates temperatures up to 500°C when properly cured. Each secondary coil has two layers (325 turns) on 14-mm o.d. quartz tubing.

The reactor is a 10-mm i.d. quartz tube, packed with approximately 3 g of Harshaw 0104 nickel–kieselguhr catalyst in a 5-cm bed and connected to a gas flow system.

In practice the reactor, the heating unit, and the primary coil remain stationary with the bed in the center of the solenoid. The secondary is mounted on a vernier drive and is moved down the length of the bed to include from 0 to 100% of the catalyst volume in one of secondary coils. The secondary signal measures the amount of reduced nickel in the coil. This signal is amplified, rectified, and read from a meter

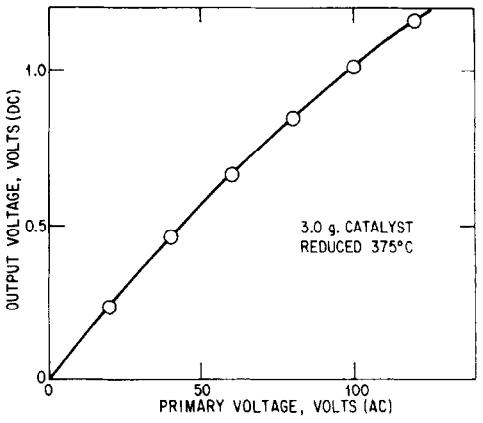

FIG. 2. Output signal as a function of primary voltage.

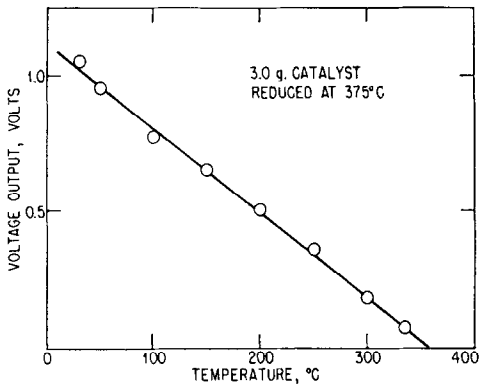

FIG. 3. Output signal as a function of temperature.

or displayed on an X–Y recorder. Figure 2 gives the output signal for a reduced bed as a function of the primary voltage. Figure 3 shows a plot of output voltage versus temperature, with the disappearance of the signal at 360°C, the Curie point of nickel. Both these observations are consistent with permeameter performance demonstrated earlier by Selwood (*4*).

The use of the moving coil permeameter in concentration profile analysis is shown in Fig. 4. It is assumed that the sulfur is adsorbed and converted to a nickel sulfide NiS_x, which is not ferromagnetic and therefore undetectable with the coil. The concentration profile is given by

$$\frac{[\mathrm{Ni}]}{[\mathrm{Ni}]_s} = f(x), \qquad (1)$$

where [Ni] is the concentration (g/cm^3) of nickel in the element dx at a position x; $[\mathrm{Ni}]_s$ is the maximum value of [Ni] and is constant over the bed length. The output voltage is zero when the end of coil is at the beginning of the bed ($x = 0$). An increasing amount of nickel enters the coil as it moves along the bed and the signal increases. At the position shown in Fig. 4(b) the end of the coil is at x and the voltage is given by

$$V = A \cdot [\mathrm{Ni}]_s \cdot \int_0^x f(x)dx, \qquad (2)$$

where A is the coil geometric factor. When the coil has moved to position $x = L$, it has encompassed the complete bed and traced the curve $V(x)$ shown in Fig. 4(c). The broken line is the equivalent line for a freshly reduced, nonsulfided bed. Normalizing,

$$\frac{V(x)}{V'(L)} = \frac{\int_0^x f(x)dx}{\int_0^L f'(x)dx}, \qquad (3)$$

where $V'(L)$ is the voltage output for the fully reduced bed and $f'(x)$ is its concentration profile. Neglecting end effects,

$$f'(x) = 1, \qquad (4)$$

and

$$\int_0^x f(x)dx = \frac{V(x)}{V'(L)} \cdot L. \qquad (5)$$

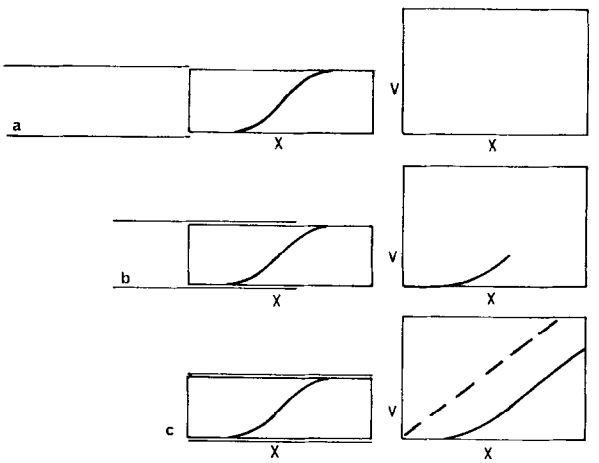

FIG. 4. Typical use of the moving coil permeameter: (a) $x = 0$; (b) integrated output at x, (c) $x = L$.

Differentiating,

$$f(x) = \frac{L}{V'(L)}\left[\frac{dV(x)}{dx}\right]_x, \quad (6)$$

$$\frac{[\mathrm{Ni}]}{[\mathrm{Ni}]_S} = \frac{L}{V'(L)} \cdot \left[\frac{dV(x)}{dx}\right]_x. \quad (7)$$

The voltage versus bed depth curve shown in Fig. 4(c) is differentiated graphically, numerically, or instrumentally to yield the relationship $[\mathrm{Ni}]/[\mathrm{Ni}]_S$. From this

$$\frac{W}{W_S} = 1 - \frac{[\mathrm{Ni}]}{[\mathrm{Ni}]_S}, \quad (8)$$

where W/W_S is the poisoning equation for the sulfur uptake.

2. *Magnetization Measurements*

Magnetization, σ, of the reduced nickel catalyst was measured with a Faraday-type apparatus described earlier (*5*). The sample was reduced *in situ* for the required time and temperature, cooled in hydrogen to room temperature and the magnetization was measured as a function of magnetic field strength up to 4500 Oe. The nickel particles in these systems are usually superparamagnetic (*4*). The saturation magnetization, σ_∞, was found from the empirical relationship (*4*, *6*):

$$\frac{1}{\sigma} = \frac{1}{\sigma_\infty} + \frac{1}{\sigma_\infty(\alpha H)^{0.9}}, \quad (9)$$

and the percentage of nickel reduced, w, from

$$w = \frac{100\sigma_\infty}{55.5}. \quad (10)$$

For low magnetic fields, the theory of superparamagnetism gives

$$d^2 = \frac{18kT}{\pi IH}\left|\frac{\sigma(H)}{\sigma(\infty)}\right|, \quad (11)$$

where d is the average particle diameter, and I is the spontaneous magnetization of bulk nickel. This procedure has been shown to yield results in agreement with chemical analysis (*7*).

3. *Catalysts*

The catalyst was Harshaw Ni 0104T, a 59% nickel on kieselguhr. Magnetization measurements indicated the nickel was 59% reduced when received from the manufacturer. Activation in hydrogen for 16 hr at 375°C resulted in a further reduction to 73% reduced nickel. This was the standard pretreatment in most of the experiments described below.

4. *Sulfiding*

The catalyst was crushed to a 20–40 mesh sample and 3 g were charged to the reactor to form a 5-cm bed. The catalyst was pretreated and the voltage-bed depth relationship determined as described above. All measurements were made at 25°C.

The nickel was sulfided with a mixture of hydrogen and the particular sulfur compound. This blend was passed over the catalyst at a flow rate, F, and temperature, T, for a given process time, t, following which the bed was quickly cooled to room temperature in flowing hydrogen. The voltage-bed distance curve was recorded, the temperature was raised to T, and the procedure was repeated. In this way, a series of curves was obtained for several values of t until the bed was completely sulfided.

The sulfur compounds were H_2S, CS_2, C_4H_4S, and $(C_2H_5)_2S$, with concentrations from 0.5 to 2.6 mole % in H_2.

5. *Catalytic Activity*

In some cases the activity for benzene hydrogenation was determined at room temperature after the voltage-bed distance measurement was made. Hydrogen was bubbled through a benzene saturator at 0°C and the conversion was determined from the benzene concentration in the feed and tail gas.

Results and Discussion

Typical results and analysis are shown in Fig. 5. The experimental points from the voltage-bed depth measurement are

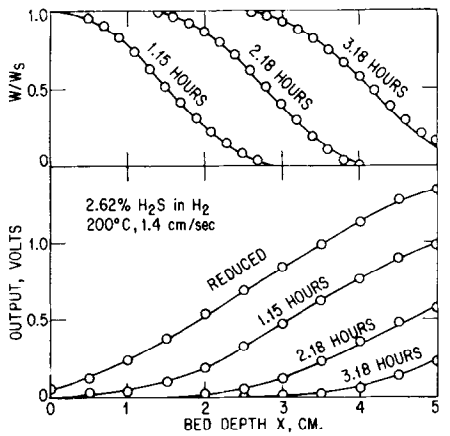

FIG. 5. Typical results from the moving coil permeameter: (lower) integrated output signals; (upper) calculated profiles.

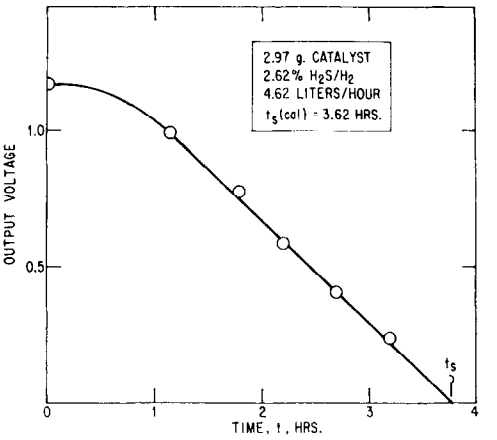

FIG. 6. Determination of t_s.

shown in the lower part of Fig. 5. These points were fitted to a linear polynomial of the form,

$$V = A + Bx + Cx^2 + \ldots Gx^6, \quad (12)$$

using a regression analysis on an IBM 360 computer. The analytical curves were differentiated according to Eqs. (7) and (8) and calculated points are plotted in the upper part of Fig. 5. Each of these sets of points was adjusted to the wave equation,

$$\frac{W}{W_s} = \frac{1 - \exp(-Nt/t_s)}{1 + \exp(-Nt/t_s)\,[\exp(Nx/L) - 1]}, \quad (13)$$

where t_s is the time for complete sulfiding of the bed. This was determined by plotting the values of $V(L,t)$ and extrapolating to t_s as shown in Fig. 6.

Equation (13) fits the computed points with a deviation of ± 0.015. Figure 5 shows the wave moving down the bed as process time increases. This is an example of a "constant pattern" zone for favorable equilibrium (*2*).

Equation (13) is the Bohart–Adams (*8*) wave equation, which may be used as a first approximation to account for the mechanism of the sulfiding reaction. In its original form the equation describes a surface reaction,

$$\frac{-d[\mathrm{Ni}]}{dt} = k_R[\mathrm{S}][\mathrm{Ni}], \quad (14)$$

but may be applied approximately to cases where either mass transfer, pore diffusion, solid phase diffusion or adsorption are limiting. In each case, the parameter, N, assumes a different interpretation since

$$N = \frac{\bar{k}L}{V}, \quad (15)$$

where $\bar{k}$ is an overall rate constant and V the linear superficial velocity of the feed. For different resistances in series

$$\bar{k} = \frac{1}{\frac{1}{k'_M} + \frac{1}{k'_P} + \frac{1}{k'_S} + \frac{1}{k'_A} + \frac{1}{k_R}}, \quad (16)$$

where $k'_M = k_M a/\epsilon$—mass transfer; $k'_P = k_P a/\epsilon$—pore diffusion; $k'_S = k_S a W_S \rho/[\mathrm{S}]$—solid phase diffusion; $k'_A = k_A W_S \rho$—adsorption; a = surface of catalyst per unit volume of reactor, ϵ = void space; and ρ = adsorbate density.

This is a model similar to the one discussed by Levenspiel for a noncatalytic reaction between a fluid and a spherical solid (*9*). Different mechanisms or combinations of mechanisms will predominate under different process conditions. In theory, it is possible to analyze the dependence of $\bar{k}$ on gas velocity, particle size, sulfur concentration, and temperature in order to establish the controlling mechanism and to evaluate the parameters. With this information extrapolation to other conditions is possible, thus facilitating the design of guard chambers and reactor beds.

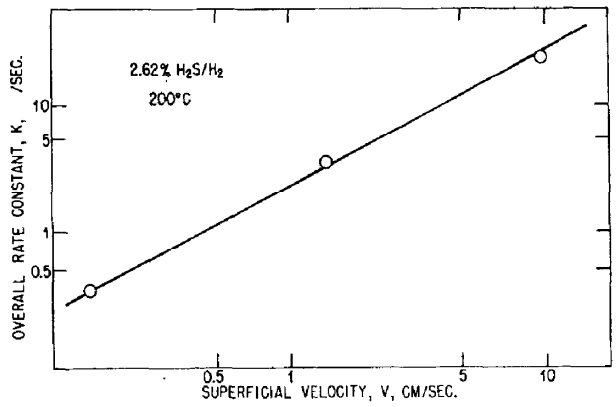

FIG. 7. Dependence of overall rate constant, $\bar{k}$, on velocity, V.

Figure 7 shows that $\bar{k}$ increases with V, suggesting film or bulk mass transfer effects. However, the power of the dependence is approximately unity rather than the one half power predicted by simplified empirical correlations (*9*). In addition, the experimental value of the mass transfer coefficient at a velocity of 1 cm/sec is 0.0105 cm/sec, whereas the calculated value is 4.20 cm/sec.

These discrepancies suggest that other factors such as axial dispersion and/or intraparticle diffusion are affecting the rate controlling process. Further measurements over a wider velocity range and with a variety of particle sizes are necessary to resolve this point.

Some insight into the prevailing mechanism is evident in the temperature dependence shown in Fig. 8. The increase of the rate constant for H_2S and C_4H_4S is greater than expected for film diffusion, indicating some reaction resistance at lower temperatures. However, $\bar{k}$ for CS_2 is almost temperature independent up to 300°C and decreases with temperature above this point. It is possible that CS_2 follows mass transfer resistance with some effects from solid phase diffusion. The curves for H_2S, CS_2, and $(C_2H_5)_2S$ coincide above 250°C, suggesting a common mechanism related to this solid phase diffusion.

Bourne *et al.* (*10*) have postulated that thiophene adsorbs and decomposes above 150°C to H_2S. The controlling mechanism may be the adsorption of the thiophene with diffusion of the H_2S through the sulfided outer layers.

Figure 9 shows a linear dependence of benzene hydrogenation activity on the amount of unsulfided nickel remaining in the bed after H_2S sulfiding at 200°C. This linear poisoning curve is consistent with

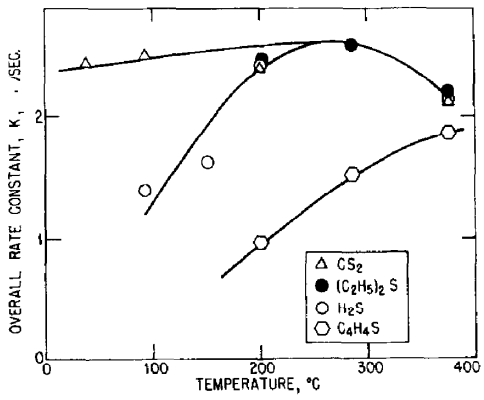

FIG. 8. Dependence of overall rate constants, $\bar{k}$, on temperature; for H_2S, CS_2, $(C_2H_5)_2S$ and thiophene.

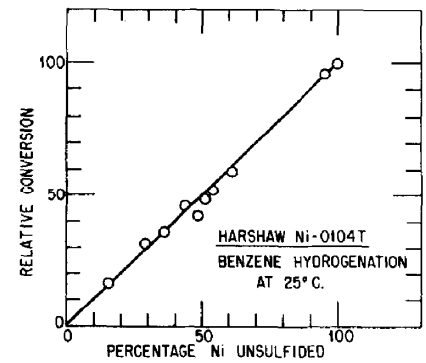

FIG. 9. Benzene hydrogenation on the sulfided bed.

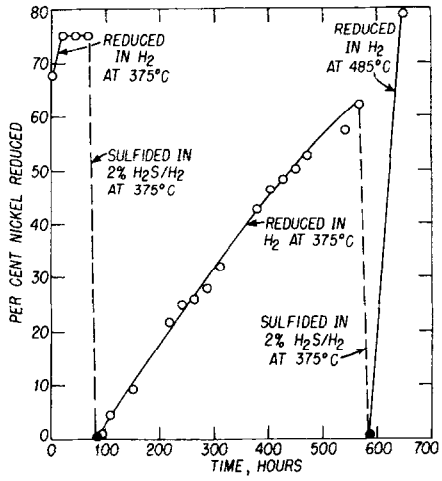

FIG. 10. Magnetic measurements on sulfided and regenerated nickel catalyst.

the prediction of Anderson and Whitehouse (*11*) for a strongly and rapidly adsorbed poison. Furthermore, since benzene hydrogenation is a good measure of a clean nickel surface, this result confirms that the nickel in the bed ahead of the mass transfer zone is unpoisoned by any adsorbed sulfur.

A series of regeneration studies are illustrated in Fig. 10. These measurements were made with the Faraday balance as described above. The catalyst was sulfided at 375°C following the usual pretreatment. Regeneration was very slow at 375°C but increased rapidly at 485°C. Figure 11 shows the results of a further series of regenerations at higher temperatures. Both the Faraday balance and the permeameter were used under identical conditions of particle size, gas velocity, and temperature. The two techniques yielded data which follow the same time dependence, suggesting that identical mechanisms prevailed during the experiments.

Figure 12 is an Arrhenius plot of initial rate versus reciprocal temperature. The characteristic transition from reaction to diffusional limitations is apparent by the change in the slope.

It is significant that all of the regenerated catalysts were inactive for benzene hydrogenation yet still contained from 0.5 to 5 wt % sulfur after reduction had ceased. It is well known that sulfur-poisoned nickel catalysts cannot be regenerated and that a nonreducible, inactive layer of nickel sulfide persists. Some insight into this effect has been given by Leftin and Stern (*12*) who demonstrated the existence of a nonreducible square planar sulfur compound on the surface of the sulfur-poisoned nickel catalyst.

However, the regenerated sulfur compounds may be resulfided by H_2S to give the same mass transfer zone characteristics as the fresh catalysts. Presumably, nickel guard chambers are regenerable and will continue to perform as guard chambers even though catalytic activity is destroyed.

Thiophene sulfided beds do not give the same results. Preliminary experiments have

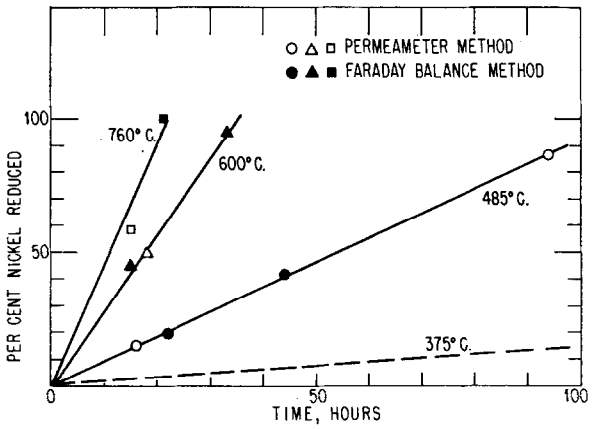

FIG. 11. Regeneration of sulfided nickel catalyst.

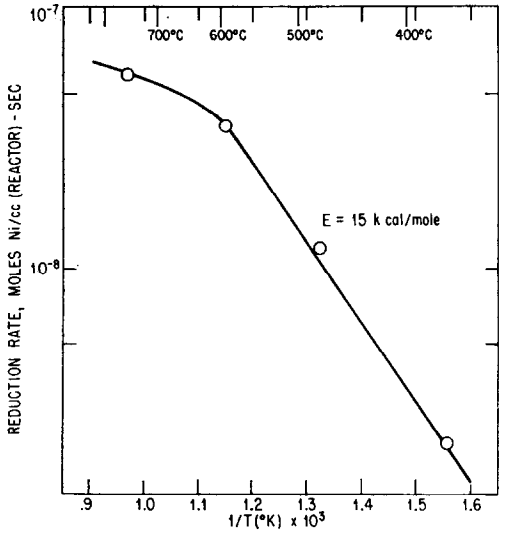

FIG. 12. Arrhenius plot of reduction rates.

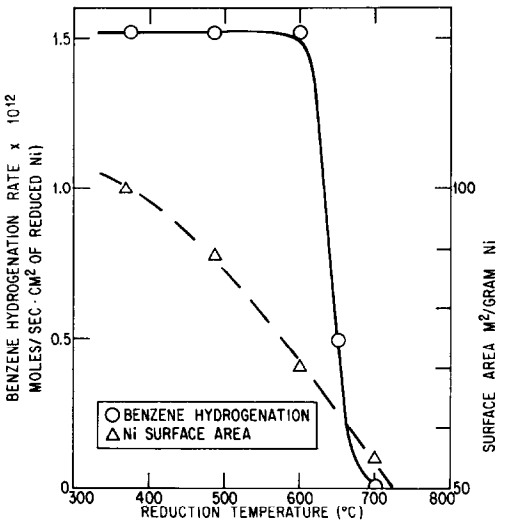

FIG. 13. Benzene hydrogenation and nickel surface for catalyst reduced at different temperatures.

shown that regenerated thiophene-poisoned beds do not retain their ability to absorb thiophene. This is, perhaps, to be expected in view of the proposed mechanism (*10*) whereby the thiophene must first be adsorbed by the nickel and decomposed before sulfiding occurs. The nickel sulfide does not have the same ability to promote this step. This aspect and other facets will be explored in a comprehensive investigation of thiophene adsorption to be reported later.

The results on the H_2S sulfided catalysts show that the higher temperatures result in the fastest regeneration. However, Schuit and Van Reijen (*6*) found adverse effects for too high a temperature of reduction. This feature was confirmed for the catalyst used in this study as shown in Fig. 13. The surface areas are based on magnetic particle size measurement assuming spherical shapes. The nickel declines in surface area for reduction temperatures from 400 to 700°C, but not with the drastic sintering so often assumed for nickel catalysts. The intrinsic benzene conversion remains constant until 600°C but decreases rapidly to zero at 700°C, in spite of the large amount of nickel surface still existing. Schuit and Van Reijen (*6*) concluded that a "skin" of some nickel-support compound covers the surface of the nickel particle, rendering it unaccessible to the reactants. This mechanism is consistent with the data in Fig. 13 which represent essentially a measurement of the real nickel surface area (magnetic particle size) versus accessible nickel surface area (benzene conversion).

The data in Fig. 13 show that 600°C is the maximum temperature at which the sulfided catalyst should be regenerated.

CONCLUSIONS

The measurement of nickel sulfide concentration profiles in sulfided nickel beds has been demonstrated with a moving coil permeameter. The shape of the profile in the mass transfer zone has been shown to fit the Bohart–Adams poisoning wave equation. The parameters of this equation when interpreted in terms of rate constants indicate chemical reaction limitations at lower temperatures (<150°C), intraparticle diffusion with some axial dispersion at intermediate temperatures (150–300°) and solid phase diffusion at high temperatures (>300°C). The behavior of thiophene is consistent with a mechanism of adsorption, decomposition, and sulfiding.

Regeneration is possible for H_2S-poisoned catalysts but only for guard chamber applications. A layer of sulfide remains at

the surface thus effectively poisoning catalytic activity. Thiophene-poisoned beds are not regenerable. Reduction of the bulk sulfide is reaction controlled below and diffusion controlled above 550°C. Reduction above 600°C is also harmful since the support forms a "skin" over the nickel surface.

Acknowledgments

The author acknowledges the assistance of Mr. S. S. Toups who constructed much of the apparatus and performed the measurements. Discussions with Dr. M. Boudart were significant during the early phases of the program.

References

1. Moison, R. L., and O'Hern, H. A., *Chem. Eng. Progr. Ser.* **24**, 71 (1959).
2. Vermeulen, T., *Advan. Chem. Eng.* **2**, 147 (1958).
3. Wheeler, A., and Robell, A. J., *J. Catal.* **13**, 299 (1969).
4. Selwood, P. W., "Adsorption and Collective Paramagnetism." Academic Press, New York, 1962.
5. Richardson, J. T., and Beauxis, J. O., *Rev. Sci. Instrum.* **34**(8), 877 (1962).
6. Schuit, G. C. A., and Van Reijen, L. L., *Advan. Catal. Relat. Subj.* **10**, 243 (1958).
7. Trzebiatowski, W., "Catalysis and Chemical Kinetics." Academic Press, New York, 1964.
8. Bohart, A., and Adams, E., *J. Amer. Chem. Soc.* **42**, 523 (1920).
9. Levenspiel, O., "Chemical Reaction Engineering." Wiley, New York, 1962.
10. Bourne, K. H., Holmes, P. D., and Pitkethly, R. C., "Proceedings of the Third Congress on Catalysis," Vol. 11, p. 1400. Wiley, New York, 1965.
11. Anderson, R. B., and Whitehouse, A. M., *Ind. Eng. Chem.* I **53**, 1011 (1961).
12. Leftin, H. P., and Stern, E. W., *J. Catal.* **6**, 337 (1967).